

Special  
Issue

# Brain-Cortex Microglia-Derived Exosomes: Nanoparticles for Glioma Therapy

Adriana-Natalia Murgoci,<sup>[a, b, c]</sup> Dasa Cizkova,<sup>[a, b, c]</sup> Petra Majerova,<sup>[b]</sup> Eva Petrovova,<sup>[c]</sup>  
Lubomir Medvecky,<sup>[d]</sup> Isabelle Fournier,<sup>[a]</sup> and Michel Salzet<sup>\*[a]</sup>

The function and integrity of the nervous system require interactive exchanges among neurons and glial cells. Exosomes and other extracellular vesicles (EVs) are emerging as a key mediator of intercellular communication, capable of transferring nucleic acids, proteins and lipids influencing numerous functional and pathological aspects of both donor and recipient cells. The immune response mediated by microglia-derived exosomes is most prominently involved in the spread of neuroinflammation, neurodegenerative disorders, and brain cancer.

Therefore, in the present study we describe a reproducible and highly efficient method for yielding purified primary microglia cells, followed by exosome isolation and their characterization. An in vitro biological assay demonstrates that microglia-derived exosomes tested on a 3D spheroid glioma culture were able to inhibit tumor invasion in time course. These results evidence that brain microglia-derived exosomes could be used as nanotherapeutic agents against glioma cells.

## 1. Introduction

The first data describing vesicles that were able to traffic between cells were published in 1983 in two distinct papers by Harding et al.<sup>[1]</sup> and Pan et al.<sup>[2]</sup> The nomenclature “exosomes” for these vesicles was established in 1989 by Johnstone et al.<sup>[3]</sup> It is difficult to make a strict classification for all extracellular vesicles (EVs), but till now exosomes were characterized as extracellular vesicles with endocytic origin, released by cells when multivesicular bodies (MVB) fuse with plasma membrane.<sup>[4]</sup> Exosome have spherical structures of 50–150 nm diameter with a lipid bilayer membrane similar with cell donor membrane, with a complex cargo represented by proteins, lipids, mRNAs, microRNAs and DNA<sup>[5]</sup> (Figure 1). Thus, the findings that EVs play a crucial role in the intercellular transport of

these molecules uncover a new view on cellular communication within the nervous system. Furthermore, recent studies in neuro-glial crosstalk have attributed an important role for extracellular vesicles exchanges in transiting mutual signals between the microglia and neurons under physiological as well as pathological conditions.<sup>[6]</sup> While neurons and astrocytes represent majority of the brain population, microglia account for roughly 12% of total brain cells. Their physiological role is maintaining homeostasis in the central nervous system (CNS) by monitoring tissue for debris and pathogens and clearing it via phagocytic activity.<sup>[7]</sup> Microglia can be activated after injury, inflammation or neurodegenerative diseases, by increasing phagocytic activity, undergoing morphological and proliferative changes, or secreting reactive oxygen and nitrogen species, pro-inflammatory chemokines and cytokines.<sup>[8]</sup> As these microglial responses contribute to CNS disease pathogenesis, research aimed on microglia-derived exosomes has gained increased interest in developing routine methods for isolation pure microglia and microglia-derived exosomes. In this context EVs have been identified as important factors in synapse assembly and plasticity, but also may play an essential role in the neuro-inflammation, in the spreading of misfolded proteins in neurodegenerative disorders, such as Alzheimer diseases (AD)<sup>[9]</sup> or even in CNS cancer (glioblastoma).<sup>[10]</sup>

So far, there is evidence that microglia-derived EVs can regulate: 1) acute inflammatory response (by converting immature IL-1 $\beta$  into a biologically active molecule),<sup>[11]</sup> 2) the excitation–inhibition balance via endocannabinoids content,<sup>[12]</sup> 3) increase synaptic vesicle release and their activity in neurons, or 4) reduce amyloid- $\beta$  levels, a neurotoxic peptide linked to AD.<sup>[13]</sup>


Even though the studies of exosomes date to at least three decades, a detailed close-up analysis of these microglia-derived

[a] Dr. A.-N. Murgoci, Dr. D. Cizkova, Prof. I. Fournier, Prof. M. Salzet  
Univ. Lille, Inserm, U-1192—Laboratoire Protéomique  
Réponse Inflammatoire et Spectrométrie de Masse-PRISM  
F-59000 Lille (France)  
E-mail: michel.salzet@univ-lille1.fr

[b] Dr. A.-N. Murgoci, Dr. D. Cizkova, Dr. P. Majerova  
Institute of Neuroimmunology  
Slovak Academy of Sciences  
Dúbravská cesta 9, 845 10 Bratislava (Slovakia)

[c] Dr. A.-N. Murgoci, Dr. D. Cizkova, Dr. E. Petrovova  
Department of Anatomy, Histology and Physiology  
University of Veterinary Medicine and Pharmacy in Košice  
Komenského 73, 041 81 Košice (Slovakia)

[d] Dr. L. Medvecky  
Institute of Materials Research  
Slovak Academy of Sciences  
Watsonova 47, 040 01 Košice (Slovakia)

 Supporting Information and the ORCID identification number(s) for the author(s) of this article can be found under:  
<https://doi.org/10.1002/cphc.201701198>.

 An invited contribution to a Special Issue on Neurochemistry: Methods and Applications

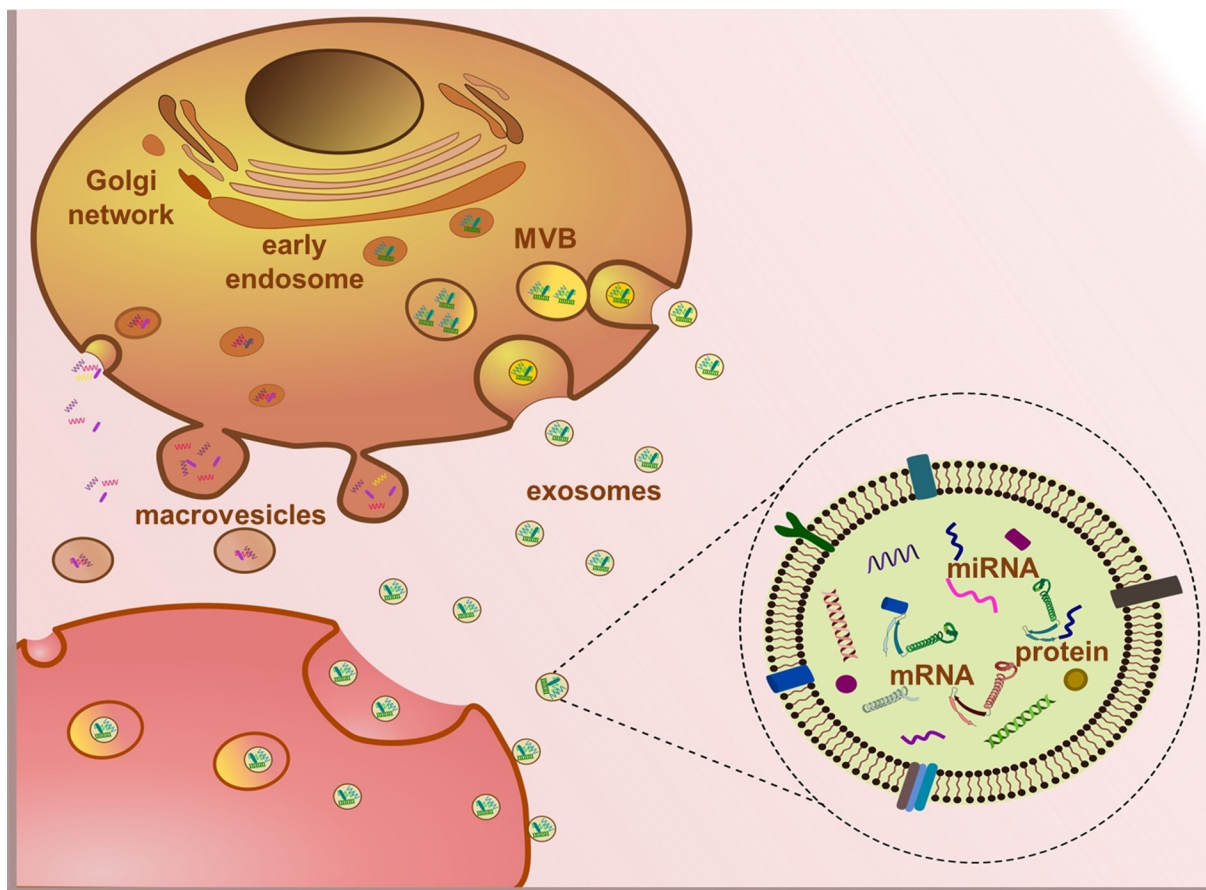


**Figure 1.** Schematic representation of exosome release and general content of an exosome. Upon MVB fusion with the plasma membrane, exosomes are set free in the extracellular space. The general cargo of exosomes is represented by proteins, lipids, mRNA, and miRNA.

EVs is still difficult, with a lot of technical issues and improvements that needs to be resolved. Therefore, in the present study, we describe a reproducible and highly efficient method of microglia-derived exosome isolation from rat neonatal cortex, followed by a battery of procedures including immunohistochemistry, SEM and nanoparticle tracking analysis, that help us to uncover their overall characteristics. We then analysed the impact of microglia derived EVs in 3D glioma model and demonstrate that these EVs suppressed invasive behaviour of cancer cells, thus may be considered as potential therapeutic agents against glioma cells.

## 2. Results and Discussion

### 2.1. Primary Rat Microglia Isolation

For primary microglia-cell culture isolation, neonatal pups at 3–4 days of age were used, as recommended by previous studies.<sup>[14]</sup> According to our preliminary data, we do not recommend using pups older ( $>P6$ ), because with aging there is a need to use additional demyelination procedure, which may decrease the final amount of obtained microglia cells (data not shown). By using standard CD11b/c (Microglia) MicroBeads, we succeed to isolate from 10 brains highly enriched microglia population containing  $1.5 \times 10^6$  cells (Figure 2). Microglia in cul-

ture show different morphological features then in vivo. While intact brain microglia are highly ramified, microglia in culture reveal round or bipolar cells morphology.<sup>[15]</sup> Thus, here we confirm that isolated primary microglial cells at 1–2 days in vitro (1–2DIV) were almost exclusively amoeboid, most frequently showing an ovoid shape with a few cells with fusiform shape at 3–4DIV (Figure 3A,B). On the other hand, heterogeneous morphology was detected in culture containing CD11b/c negative fraction, revealing bipolar or multipolar cells displaying a very neural morphology with long processes (Figure 3C,D). Microglia morphology slightly changed along in vitro maintenance from round-amoeboid shape (4DIV) to a population, including also ramified cells (7–10DIV) (Figure 4E). At last day in culture (10DIV) we have assessed efficacy of CD11b/c MicroBeads separation, by performing immunocytochemistry using antibodies against CD11b receptor (red) (Figure 4A), and Iba1 protein (green) (Figure 4B). The analyses documented that 94.19% of cells were positive for CD11b antibody and 94.34% of cells were positive for Iba1 antibody (Figure 4F), thus confirming microglia phenotype. Furthermore, double stained microglia became more heterogeneous including amoeboid shape cells and those presenting a ramified morphology, and bearing a single large lamellipodia (Figure 4E). This pattern is in line with in vitro data indicating typical morphology of primary microglia isolated by different protocols.<sup>[16]</sup> The popula-

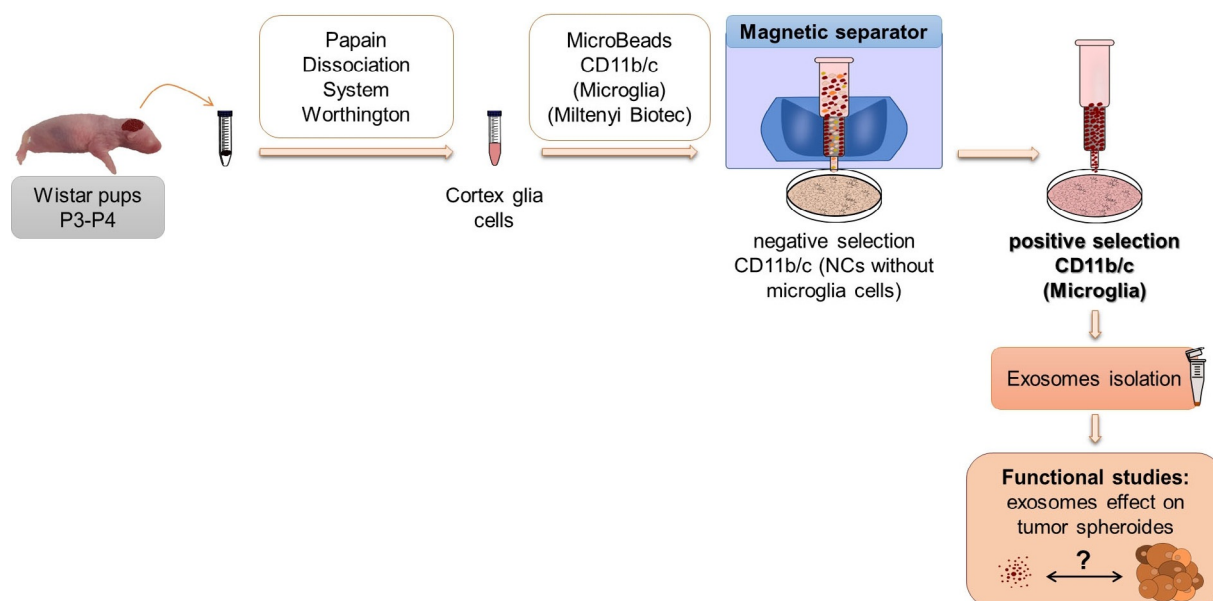


**Figure 2.** Scheme of the experiments: Neural progenitor cell isolation from a rat pup and microglia separation with specific CD11b/c (Microglia) MicroBeads, followed by exosome isolation and functions studies.

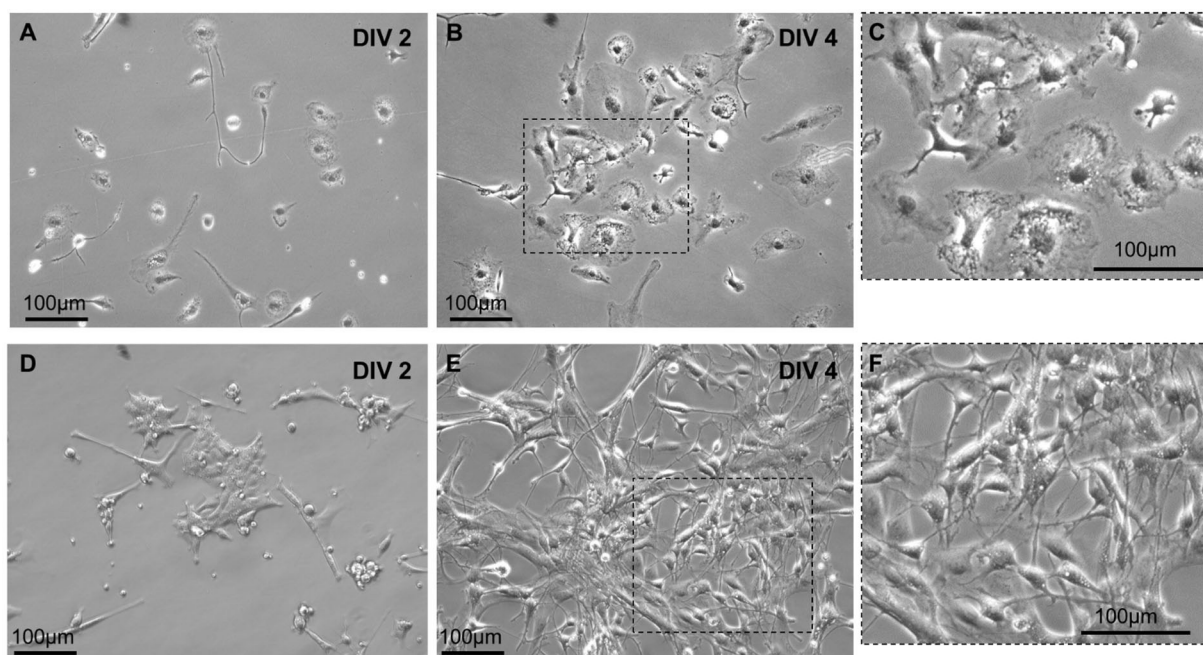


**Figure 3.** Microglia cells (A, B, C—higher magnification for box area) and cells negative for CD11 b/c (D, E, F—higher magnification for box area) in culture. A different cell morphology starts to be visible after two days in vitro (DIV) and is clear after four DIV. Scale bars: 100 μm.

tion of NCs (CD11b negative fraction) contained mainly astrocytes and rarely oligodendrocytes (Supplementary Figure 1A,B). We did not detect neurons, most probably due to incubation in basic culture medium (lacking important neuronal supplements) which did not support neuronal survival (Supplementary Figure 1C).

## 2.2. Microglia Exosome Isolation

Various procedures for exosome isolation have been published, which are based on different biophysical and biochemical properties of EVs, such as size, mass density, shape, charge, or antigen exposure.<sup>[16,17]</sup> Each method presents advantages and disadvantages, and each protocol should be adapted according to function of EVs origin and experiment type.<sup>[18]</sup> Presently, there is no universal protocol available for exosomes isolation from various tissues. However, ultracentrifuge approach is con-



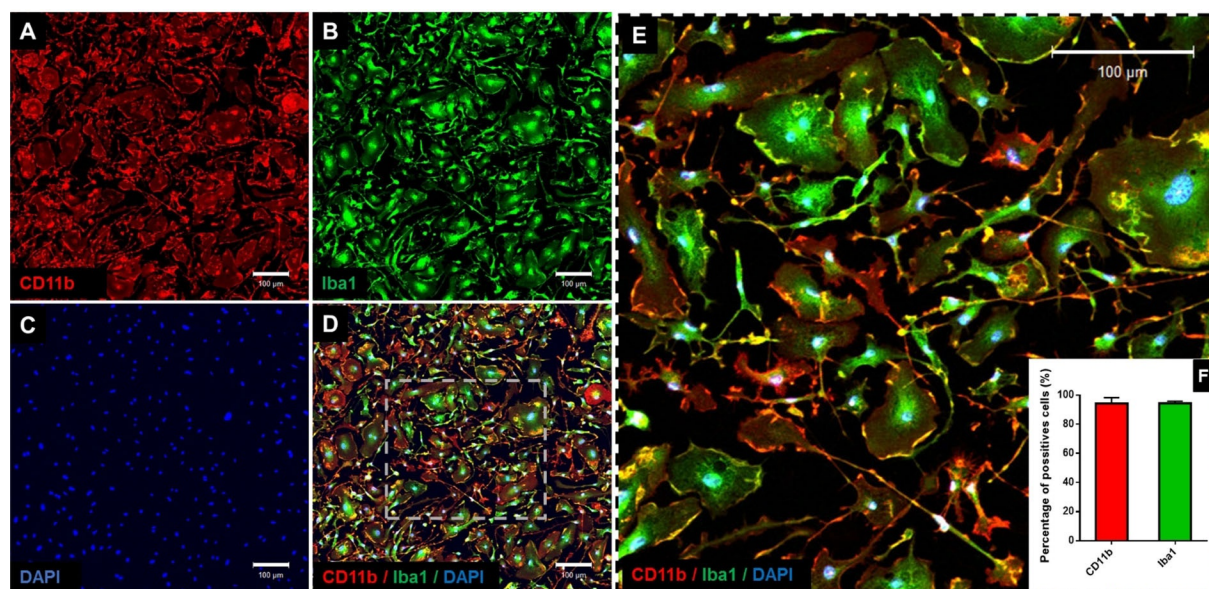


**Figure 4.** Double immunocytochemistry for cortex microglia cells to establish the efficiency of CD11 b/c MicroBeads microglia separation: (A) anti-CD11b (red) and (B) anti-Iba1 (green), both markers for microglia cells, (C) DAPI (blue) stain for cell nucleus (D) merge of all three microscopic images, (E) higher magnification for box area. Scale bars: 100  $\mu$ m. (F) The percentage of total positive cells for CD11b antibody and Iba1 antibody.

siderate as gold standard of EVs isolations because it is easy to be used, requests a very little technical expertise and finally no sample pre-preparation is needed.<sup>[19]</sup> Therefore, for microglia exosome isolation, multiple centrifugation steps were used to eliminate debris and other macro vesicles, with final ultracentrifugation steps using Optima XPN80, Ultracentrifuge—Beckman Coulter with 70.1 Ti rotor, to recuperate exosome pellet (Figure 5). Many previous studies have included this strategy for exosomes isolation derived from urine,<sup>[20]</sup> serum<sup>[21]</sup> and cerebrospinal fluid.<sup>[22]</sup> Identical procedure as for microglia exosomes, was used for isolation of NCs-derived exosomes. Once exosomes were isolated, we have continued by performing their characterization, involving, fluorescent microscopy, Scanning Electron Microscope (SEM) and NanoSight.

### 2.3. Microglia Exosome Labelling with PKH67

Exosomes are lipid-membrane-bound vesicles, released by cells when MVB fuse with plasma membrane, so they carry molecular constituents of their cell origin as lipids drafts and membrane proteins.<sup>[23]</sup> Because of this, it is possible to track exosomes by labelling them with PKH67 green fluorescent cell linker, which uses a specific membrane-labelling technology to stably incorporate a green fluorescent dye with long aliphatic tail (PKH67) into the lipid regions of the cell membrane.<sup>[24]</sup> The exosomes expressing green fluorescence were visible by 100 $\times$  objective and additional 1.5 $\times$  with Nikon Ti-Fluorescence microscope (Figure 6A,B). We could observe individual vesicles of 100–200 nm diameter as well as larger clusters expressing fluo-

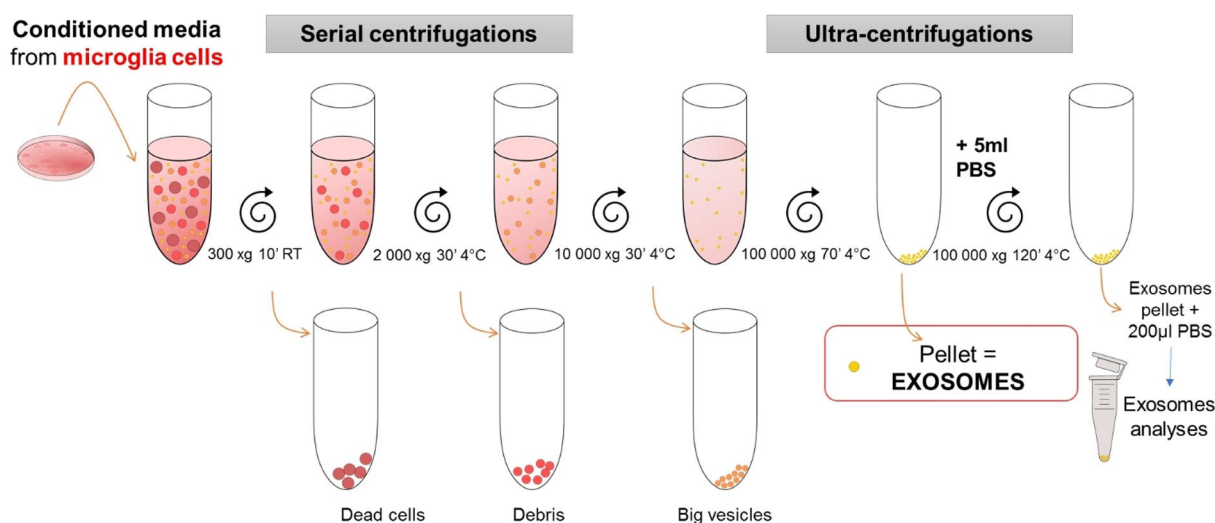


**Figure 5.** Schema of exosome isolation. The conditioned medium from microglia cells was recovered and centrifuged using different speed steps, ending with ultra-centrifugation at 100 000xg for 70 min.

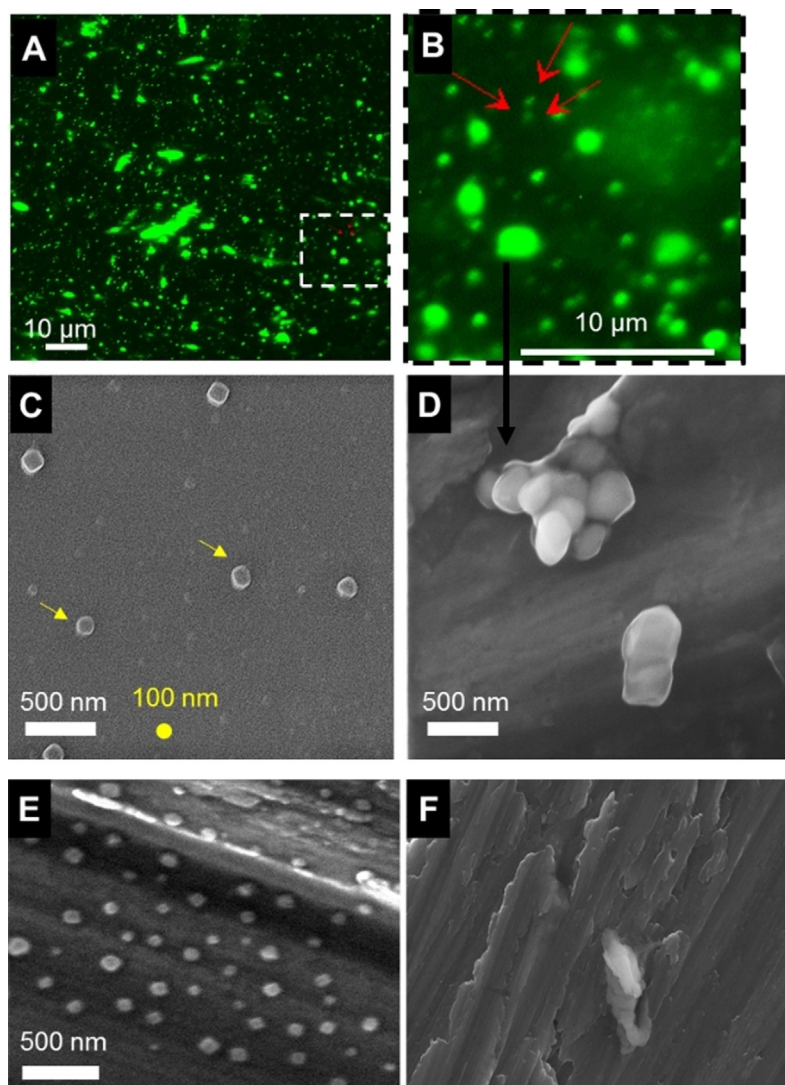


**Figure 6.** Fluorescent microscope characterisation (A and B—higher magnification for box area), SEM analyses for microglia exosomes (C and D), SEM analyses for NCs exosomes (E). Exosomes were purified from microglia cells and subsequently labelled with the lipophilic dye PKH67. Labelled exosomes can be observed at fluorescent microscope with objective  $100\times$  + oil. Multi-exosome clusters observed at fluorescent and SEM (B and D). Negative control for SEM analyses (F). The yellow arrows indicate vesicles which have approx. 100 nm diameter. Scale bars: 10  $\mu\text{m}$  (A and B), 500 nm (C and D), 100 nm perimeter (C—yellow dot).

rescence ranging  $\approx 500$  nm (Figure 6B). Representative images of labelled exosomes confirm that this procedure has some limitations due to the exosomes-derived fluorescence signal visualisation via routine fluorescence microscopy. Thus PKH labelling was in our hands moreover general procedure able to identify the presence of exosomes in the sample, and could be successfully used for additional flow cytometry analyses or for exosome uptake studies.<sup>[25]</sup>

#### 2.4. Exosome Characterisation Using Scan Electron Microscopy

We further examined the size and morphology of microglia-derived exosomes by performing field-emission scanning electron microscopy analyses (SEM) (Figure 6C–F). The SEM images indicated the presence of a homogeneous population of exo-

somes with diameters of 100–150 nm. Exosomes appeared almost exclusively round or cup shaped vesicles (Figure 6C). In rare cases we could identify multi-exosome clusters of about 500 nm diameter (Figure 6D). Furthermore, we have identified higher amount of exosomes derived from NCs (enriched astrocytes), which correlate with higher number of primary cells used for isolation. Interestingly they were homogeneously distributed revealing round shaped vesicles of  $<100$  nm (Figure 6E). In the negative control, representing FBS free conditioned media without exosomes, we did not detect any type of vesicles (Figure 6F). Taken together, these findings confirm the presence and purity of microglia derived exosomes in our preparations and are in line with similar studies uncovering exosomes characteristics derived from different cells.<sup>[26]</sup>

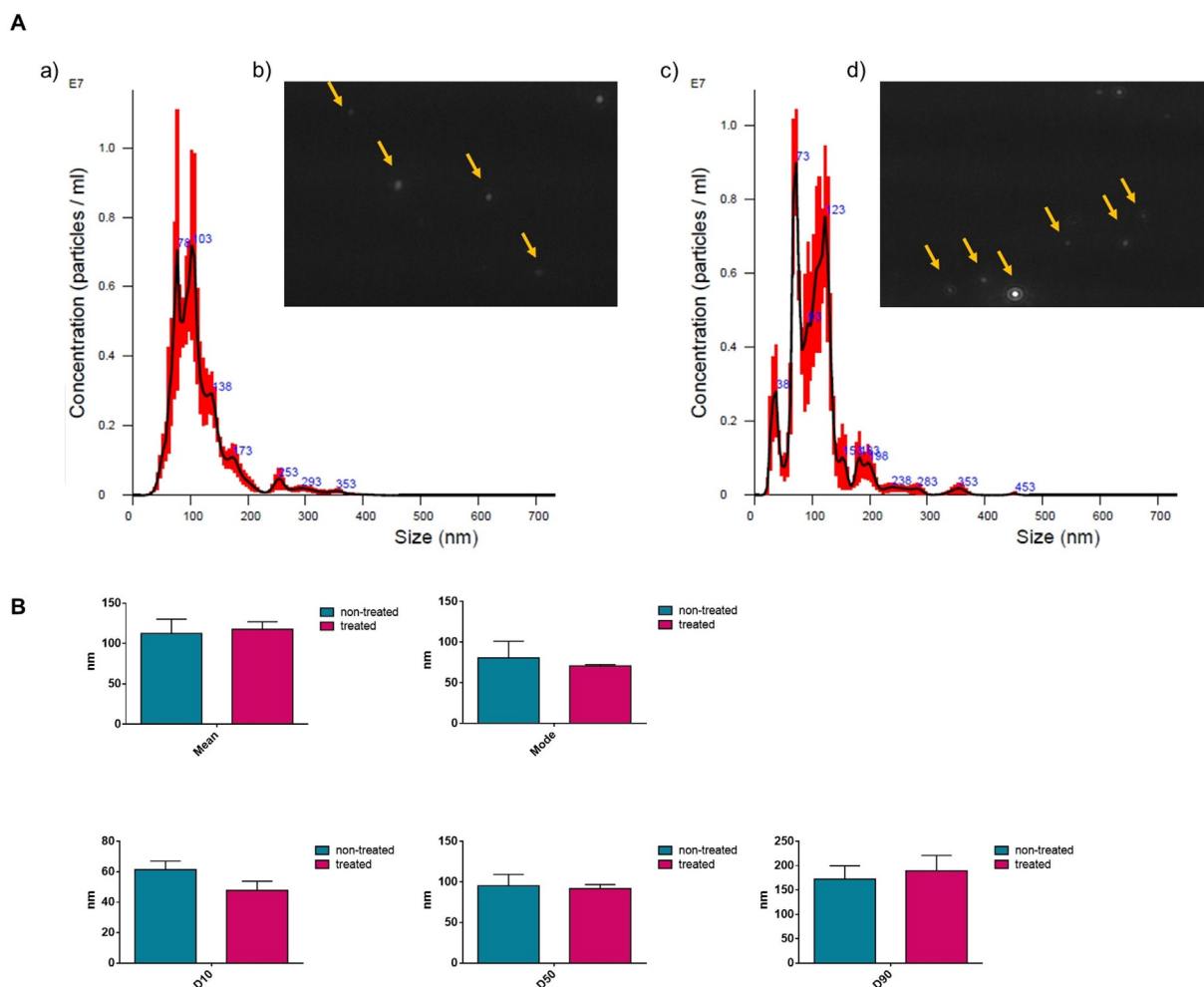


**Figure 7.** Nanoparticle tracking analysis (NTA) size distribution profiles (A) for non-treated cortex microglia exosomes (a) with the corresponding NTA video frame (b) and for LPS-treated cortex microglia exosomes (c) with the corresponding NTA video frame (d). Yellow arrows indicate EVs particles during NTA analyses. Each particle is recorded, and the size is calculated in function of the rate of the particle movement using the Stokes-Einstein equation. (B) Statistical results regarding the particles diameter ( $n=3$ ). Particle size distributions are D-Values (D10, D50 and D90) which are the intercepts for 10%, 50% and 90% of the cumulative mass.

## 2.5. Nanoparticle Tracking Analysis for Microglia Exosomes

Characterization of isolated microglia-derived exosomes was completed by nanoparticle tracking analysis (NTA) (Figure 7). Measurements with Malvern NanoSight NS300 instrument (Figure 7Aa) showed that the isolated particles from the individual three samples of non-treated microglia, were consistently within the expected size range for exosomes, revealing diameter mean of  $112.46 \pm 17.86$  nm, and diameter mode  $80.56 \pm 20.61$  nm (Figure 7Ab). The concentration of exosomes released by  $5 \times 10^5$  microglia cells was established to  $27.5 \times 10^7 \pm 6 \times 10^7$  particles (Figure 7Aa, Supp. Video 1) and for LPS-treated microglia the concentration measured was  $36.1 \times 10^7 \pm 2.1 \times 10^7$  particles secreted by  $5 \times 10^5$  microglia cells (Figure 7Ac, Supp. Video 2). After LPS treatment, the mean of the exosome size is around  $117.6 \pm 9.39$  nm which is in line with the ones in control (Figure 7B). However, slight differences occurred due to the higher proportion of small diameter particles  $< 100$  nm and those of larger size  $100 \text{ nm} <$  following

LPS treatment (Figure 7B). In conclusion, primary microglia responded to LPS stimulation by the enhanced release of exosomes ranging between 50–200 nm.

## 2.6. Microglia Exosome Effect on Glioma Cells

To confirm that the exosomes isolated have a real biological effect, we performed anti-tumoral screening based on a 3D spheroid culture system. Glioma spheroids were generated using C6 glioma cell line and were cultured for 6 days in a collagen matrix containing or not microglia exosomes (Figure 8A, Supp. Figure 2). Cell invasion out of the spheroid was monitored by digital photography. Images were acquired from day 0 to day 6 (day 0=time of embedding in collagen). Four images were taken from each spheroid, one per each corner, and analysed with Caladialac software to quantify spheroids invasion areas according to recent study.<sup>[27]</sup> Invasion and spheroid areas are normalized for each day to the invasion and spheroid areas measured at day 0. These normalized data are



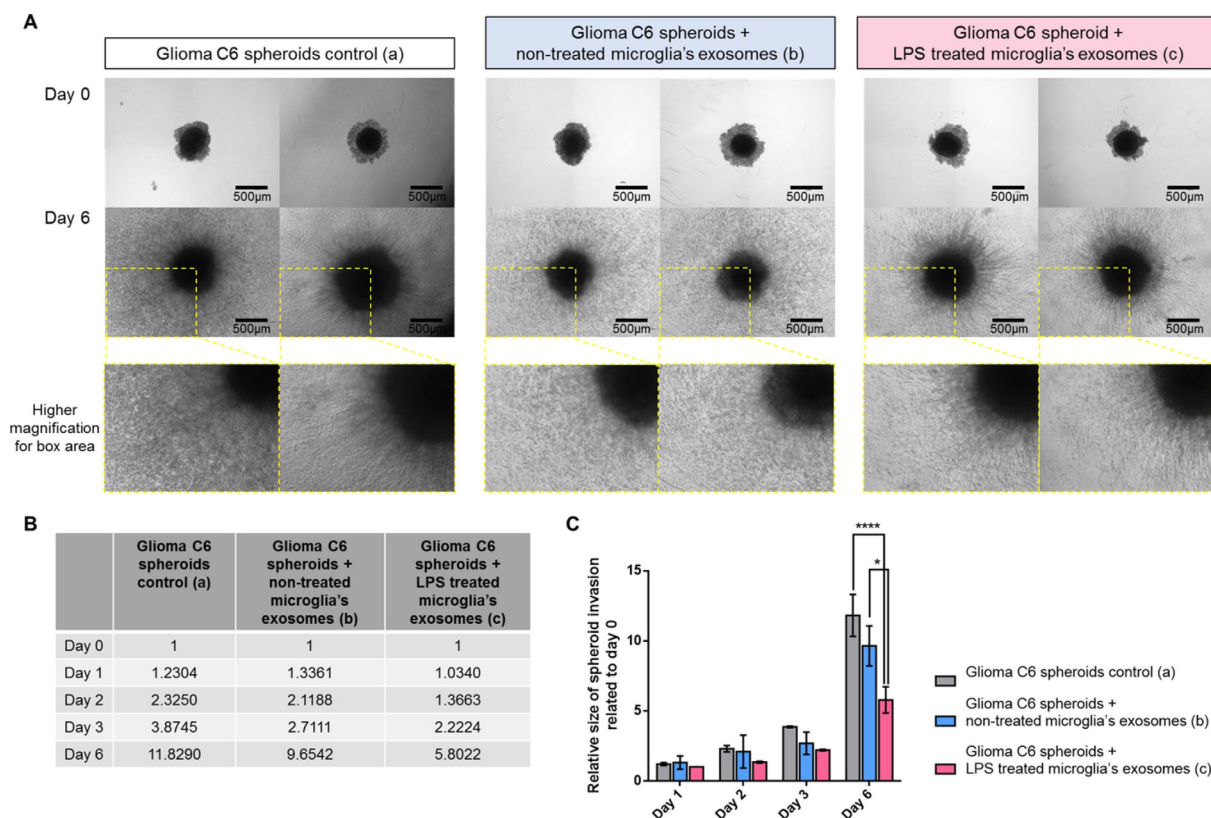


**Figure 8.** Microglia exosome effect under glioma spheroids: (A) Representative images of the invasion of C6 spheroids in the collagen matrix at day 0 and day 6. Spheroids are in the absence (a) and in the presence of exosomes released by microglia cells not treated (b) or treated 24 h with  $500 \text{ ng mL}^{-1}$  LPS (c). All images were acquired with an inverted light microscope at  $5\times$  magnification. Scale bar:  $500 \mu\text{m}$ . (B) Relative size of spheroids in days 1, 2, 3 and 6 reported to day 0. (C) Graphic representation showing ratio of C6 area invasion during treatment with microglia exosomes at each time point. \*Significant differences between C6 spheroids not treated and C6 spheroids treated with exosomes released by microglia cells ( $P \leq 0.05$ ) by 2way ANOVA test.

reported as relative size to day zero. Relative size of day 0 thus equal 1 (Figure 8B). Compared to control (Figure 8Aa), or to non-treated microglia derived exosomes ( $500 \text{ ng mL}^{-1}$  LPS) (Figure 8Ab), the ones derived from LPS-treated microglia cells clearly shown a reduction of glioma cells invasion in the collagen matrix 6 days after treatment (Figure 8Ac). A statistical significant effect of more than 50% was visible at 6 days for spheroids co-cultured with exosomes derived from LPS stimulated microglia, suggesting that these EVs contain factors (proteins or miRNA) exhibiting an anti-tumoral properties (Figure 8B,C). These results clearly stated that the isolation protocol was appropriate to obtain EVs with specific biological activity that may be used for further in vitro or in vivo experiments. The explanation for this anti-tumoral activity is unclear but it could be linked to miRNAs and its possible modulatory role for expression of genes involved in biological processes. Particularly, some members of the miR-16 family are capable of inducing cell-cycle arrest and acting as potent tumor suppressors.<sup>[28–30]</sup> This mechanisms was confirmed in recent study which showed that exosomes from plasma of malaria-infected hosts reduced tumor via suppressed angiogenesis through overexpression of the miRNA.<sup>[31]</sup>

### 3. Conclusions

In the present study, we have introduced a two-step procedure for the isolation of primary rat microglia-derived exosomes sharing biological activity. Firstly, by using standard CD11b/c (Microglia) MicroBeads, we succeed to isolate highly enriched microglia population. Afterwards, the ultracentrifugation approach enabled us to obtain efficient concentration of exosomes released by non-treated microglia cells, which after LPS stimulation increased ( $27.5 \times 10^7$  and  $36.1 \times 10^7$  particles secreted by  $5 \times 10^5$  microglia cells, respectively). Furthermore, we have identified a slightly broader scope of exosomes size after stimulation. Thus, also proportion of smaller and larger sized exosomes were detected. However, when comparing the average values of overall data, these particles correlated with controls and fulfilled the size range of EVs characteristics. Another import advantage of the ultracentrifugation procedure was, that we obtained a high quality of exosomes that remained their biological properties. Thus, LPS stimulated microglia cells derived exosomes in comparison to controls, revealed anti-cancer activities towards rat glioma cells using 3D spheroids. Fifty percent growth inhibition was registered with these LPS treated microglia exosomes at 6 days. We recently performed similar experiments with rat lung resident macrophages from NR8282 cells line in which we knock down the proprotein con-

vertase PC1/3 known to be involved in the regulation of inflammatory cytokines secretion.<sup>[32–35]</sup> We established in PC1/3-KD cells that intracellular trafficking is modified and EVs are concentrated in the cells. Activation by LPS<sup>[35]</sup> or sterile stimulation by Paclitaxel (Duhamel et al. personal data., 2017) induce the release of these EVs sharing anti-tumoral activities. In that context, exosomes isolated from PC1/3 KD cells treated with Paclitaxel also suppressed tumor invasion on C6 glioma cell. In both conditions, a fold change of  $1/2$  is registered with the treated glioma cells with exosomes issued from either LPS-treated microglia or Paclitaxel treated PC1/3-KD macrophages. These results open the door of novel therapy combining exosomes from different cellular origins for synergic effects. In that context, we can suggest that exosomes can be used as nanoparticles to target a human tumour alone or by introducing them in immune cells for immuno-therapy by shaping them as issued from human cells. In the near future, we will combine EVs of rat LPS activated microglia with the ones issued from LPS or Paclitaxel rat PC1/3 KD macrophages to human macrophages in order to modify them either directly into the tumor or by cell therapy. Taken together, the whole our data shown that EVs are novel therapeutic agents that can be used in oncology but not only.

## Experimental Section

### Animals

The study was performed with the approval and according to the guidelines of the Institutional Animal Care and Use Committee of the Slovak Academy of Sciences and with the European Communities Council Directive (2010/63/EU) regarding the use of animals in Research, Slovak Law for Animal Protection No. 377/2012 and 436/2012. All animal experiments were carried out according to the institutional animal care guidelines and in conformity to international standards (Animal Research: Reporting of In Vivo Experiments guidelines), and they were approved by the State Veterinary and Food Administration of the Slovak Republic (Ro-4429/16-221m) and by the Ethics Committee of the Institute of Neuroimmunology, Slovak Academy of Sciences.

Wistar rat pups P3-P4 ( $n=10$ ) were selected for cortex isolation. Hypothermia was used to induce anaesthesia in neonatal rats by placing them in a latex glove and immersing them in crushed ice for 2–5 min. After complete blockage of neuronal transmission, pups were decapitated with forceps. The brain was extracted into Petri dish with sterile DMEM with 2% antibiotics and all the meninges were manually removed (Supp. Video 3, Figure 2).

### Cells and Culture Conditions

The cortex was cut into pieces and transferred into a new tube; the NCs were dissociated by using Papain Dissociation System (Worthington Biochem. Corp., NJ, USA). Microglia cells were then separated from single-cell suspension by MACS<sup>®</sup> Technology using CD11b/c (Microglia) MicroBeads (Miltenyi Biotec Inc., CA, USA) according to the manufacturer's instructions. The cells were counted using EVE<sup>™</sup> Automatic Cell Counter and optimal volume of rat CD11b/c MicroBeads was added (20  $\mu$ L of CD11b/c (Microglia) MicroBeads per  $10^7$  total cells). After 30 min incubation in dark at 4 °C, microglia cells were separated by positive selection of CD11b/

c antibody microbeads attached to microglia from other cells (astrocytes, oligodendrocytes, neurons) using a magnetic field. The isolated primary microglia cells ( $1.5 \times 10^6$ ) were incubated in cell culture flasks pre-coated with poly-L-lysine 50  $\mu$ g mL<sup>-1</sup> (Sigma) containing Dulbecco's Modified Eagle Medium/Ham's Nutrient Mixture F-12 (DMEM/F12, 1:1) (BIO SERA, BioTech, Bratislava, SK) supplemented with 10% of fetal bovine serum (FBS) (GE Healthcare, Biowest, South America), 1% antibiotics (10,000 units mL<sup>-1</sup> penicillin, 10,000  $\mu$ g mL<sup>-1</sup> streptomycin, Invitrogen, Thermo Fisher Scientific), 1% L-glutamine (Sigma), 10% B27 Supplement (Gibco), 20 ng mL<sup>-1</sup> human recombinant basic fibroblast growth factor (bFGF, PeproTech) and 20 ng mL<sup>-1</sup> mouse recombinant epidermal growth factor (EGF, PeproTech), 10% N2 Supplement (Gibco, Thermo Fisher Scientific) in a humidified atmosphere with 5% CO<sub>2</sub> at 37 °C during 7–10 days. The cells negative for CD11b/c (astrocytes, oligodendrocytes, neurons), indicated as neural cells (NCs), were also recovered and cultivated in complete medium DMEM/F12 supplemented with 10% FBS and 1% antibiotics. Cells were cultivated in a humidified atmosphere with 5% CO<sub>2</sub> at 37 °C for 7–10 days.

The rat C6 glioma cell line was kindly provided by Prof. Dr. Bernd Kaina (Institute of Toxicology, University Medical Center, Mainz, Germany). C6 cells were cultured in high-glucose Dulbecco's Modified Eagle's Medium (DMEM) and supplemented with 10% heat-inactivated fetal bovine serum, 1% L-glutamine (2 mM) and 1% gentamicin (50 units per mL), all from Sigma-Aldrich. This medium is referred to as complete DMEM (cDMEM).

### Immunocytochemistry

Cells were fixed with acetone/ethanol (4/1) for 10 min at 4 °C. After incubation with blocking buffer, 5%BSA in phosphate buffered saline (PBS) for 60 min at room temperature (RT), the cells were washed 3 times with PBS and incubated O/N at 4 °C with primary antibody anti-Iba1 (1:500, rabbit polyclonal antibody; Wako Pure Chemical Industries, Osaka, Japan) and in the same time with anti-CD11b (1/200, mouse monoclonal antibody; MCA275XZ, AbD Serotec, Oxford, United Kingdom) both diluted in PBS + 5%BSA. Day after cells were washed 3 times and incubated 2 h, at RT, in the dark, with the secondary fluorescent antibodies, Alexa Fluor 488 goat anti-rabbit IgG (1/2000, Invitrogen) and Alexa Fluor 546 goat anti-mouse IgG (1/2000, Invitrogen), diluted in PBS + 5% BSA. For nuclear staining, we used 4-6-diaminidino-2-phenylindol (DAPI) (1:200, Molecular Probes, Eugene, OR). Labelled cells were observed under a fluorescence microscope confocal microscope Zeiss LSM710 (software Zen10). Using ImageJ 1.51 n software cells from three different microscopic fields (848.53  $\times$  848.53  $\mu$ m)/per condition were counted and the number of cells positive for CD11b and for Iba1 antibody was calculated as a percentage reported to the total number of cells.

### Exosome Purification Protocol

Confluent populations of microglia cells ( $\approx 5 \times 10^5$  cells) were incubated in DMEM/F12 in six well plates without FBS for 24 h to obtain cell-conditioned media (CM) free of FBS. Afterwards, the CM were cleared of cells and debris by centrifugation at 350  $\times$  g for 10 min, 4 °C followed by filtration with nylon filter membranes, pore size 0.2  $\mu$ m. This was followed by subsequent steps of centrifugation and ultracentrifugation to pellet microglia-derived exosomes. Membranes and debris were discarded from the CM by centrifugation for 30 min at 2000  $\times$  g at 4 °C. Then the withdrawn



supernatant was centrifuged at  $10000\times g$  for 30 min,  $4^{\circ}\text{C}$  to remove ectosomes and larger vesicles and followed by ultracentrifugation (Beckman Optima XPN80 Ultracentrifuge, USA) at  $100000\times g$  for 70 min,  $4^{\circ}\text{C}$ . The pellet was washed in PBS to eliminate contaminating proteins and re-ultracentrifuged at  $100000\times g$  for 120 min,  $4^{\circ}\text{C}$ . The exosomes pellet was stored at  $-20^{\circ}\text{C}$ .

## Exosome Analyses

### Exosome PKH Labelling

Isolated exosomes were labelled with PKH67 dye (Sigma, Germany) according to the manufacturer's instructions. Briefly, exosome pellets were resuspended in 50  $\mu\text{L}$  particle-free phosphate buffer (PB). Separately, 500  $\mu\text{L}$  Diluent C was mixed with 4  $\mu\text{L}$  PKH67. The exosome suspension was mixed with 50  $\mu\text{L}$  of stain solution and incubated for 30 min at RT in the dark. The PKH labelling reaction was stopped by adding an equal volume of 100  $\mu\text{L}$  FBS free exosomes (FBS was depleted of exosomes by ultracentrifugation at  $100000\times g$  for 120 min at  $4^{\circ}\text{C}$ ). Then labelled exosomes were washed with PB and the pellet was recovered after ultracentrifugation at  $100000\times g$  for 120 min,  $4^{\circ}\text{C}$ . Exosomes pellet was recovered with 30  $\mu\text{L}$  PB and 5  $\mu\text{L}$  solution were transferred on glass slides and analysed by Nikon fluorescent microscope (Nikon Eclipse Ti-S) by using 100x oil objective.

### Scanning Electron Microscopy (SEM)

The exosomes were fixed with 2.5% glutaraldehyde (Sigma-Aldrich, Germany) in PBS for 24 h at RT. The fixed exosomes were dehydrated with an ascending sequence of ethanol solutions (70%, 80%, 99%). After evaporation of ethanol, the samples were dried at room temperature. Exosome pellets were dispersed in 20  $\mu\text{L}$  ethanol (absolute, analytical grade, Merck) and 5  $\mu\text{L}$  suspension was dropped on Al substrate (polished with SiC paper 800). After ethanol evaporation, the thin carbon film (about 13 nm thickness, JEOL FC-TM20 Thickness Controller) was deposited on Al substrate using JEOL JEE-420T Vacuum Evaporator. The morphology of exosomes was observed by a field emission scanning electron microscopy (JEOL FE SEM JSM-7000F).

### Nanoparticle Tracking Analysis (NTA)

Suspensions containing vesicles were analysed using a NanoSight LM 10 instrument (Merkel technologies LTD., UK) to characterize the size and concentration of the exosomes. Each sample was diluted in particle-free PBS (1:100), and introduced into the sample chamber using a syringe pump with a constant flow rate. Five video recordings, of 60 s each were initiated. For this analysis, a monochromatic laser beam at 488 nm was applied to the dilute suspension of vesicles. Particle movement was analysed by NTA software (version 3.2, NanoSight). NTA post-acquisition settings were optimized and kept constant between samples, and each video was then analysed to give the mean, mode, and median vesicle size together with an estimation of particles concentration. Each sample was analysed in triplicate ( $n=3$ ).

### Spheroid Generation and Embedding in a Collagen Matrix

3D glioma spheroids were generated following the protocol developed by Anne Régner-Vigouroux team.<sup>[36]</sup> In brief C6 rat glioma cells were resuspended in cDMEM at the final concentration of

12500 cells in 200  $\mu\text{L}$ . Cells (200  $\mu\text{L}$  per well) were distributed in flat 96-well low attachment surface plates (Corning®). Plates were incubated at standard culture conditions for 96 h. The newly formed C6 cell spheroids were then implanted in the center of each well of a 24-well plate coated with a  $2.2\text{ mg mL}^{-1}$  collagen mixture (one spheroid per well in 400  $\mu\text{L}$  of collagen mixture per well). The collagen mixture was prepared by mixing 2 mL of PureCol® bovine collagen type I solution ( $3\text{ mg mL}^{-1}$ ; Advanced BioMatrix) with 250  $\mu\text{L}$  of 10X minimal essential medium (MEM) (Sigma-Aldrich) and 500  $\mu\text{L}$  of sodium hydroxide 0.1 M. After cell spheroid embedding, the plate was incubated for 30 min at standard culture conditions to solidify the gels. Thereafter 400  $\mu\text{L}$  of cDMEM was overlaid on the collagen matrix in each well. The complete system was incubated for a total of 6 days.

### Co-culture of Exosome Microglia with C6 Spheroids

Primary microglia cells (Innoprot P10304) were treated or not with 500 ng lipopolysaccharides (LPS) (Sigma, Escherichia coli O127:B8) for 24 h. The conditioned medium was recovered, and exosomes isolated as was described before. The exosomes pellet was resuspended in alfa MEM 10X, filtrated with 0.20  $\mu\text{m}$  filter and analysed with a NanoSight NS300 instrument (Malvern) to determine exosomes in each condition. An equal quantity of exosomes was added to the collagen mixture as described above. The collagen mixture containing EVs was distributed in 24-well plates for embedding of C6 spheroids as described above. Experiments were done in duplicate ( $n=2$ ).

## Acknowledgements

This research was supported by a collaboration between the PRISM and grants from Ministère de L'Education Nationale, L'Enseignement Supérieur et de la Recherche, INSERM, and University de Lille 1 (ANM), APVV 15-0613 (DC), Stefanik SK-FR-2015-0018 (DC, MS), ERA-NET AxonRepair (Neuron9-FP-030).

## Conflict of interest

The authors declare no conflict of interest.

**Keywords:** central nervous system • exosomes • extracellular vesicles • microglia cells • nanoparticles

- [1] C. Harding, *Eur. J. Cell Biol.* **1984**, 35, 256–263.
- [2] B.-T. Pan, R. M. Johnstone, *Cell* **1983**, 33, 967–978.
- [3] R. M. Johnstone, A. Bianchini, K. Teng, *Blood* **1989**, 74, 1844–1851.
- [4] C. Théry, L. Zitvogel, S. Amigorena, *Nat. Rev. Immunol.* **2002**, 2, 569–579.
- [5] C. Théry, M. Ostrowski, E. Segura, *Nat. Rev. Immunol.* **2009**, 9, 581–593.
- [6] C. Fröhlich, D. Fröhlich, W. P. Kuo, E.-M. Krämer-Albers, *Front. Cell. Neurosci.* **2013**, 7, 182.
- [7] D. P. Schafer, B. Stevens, *Cold Spring Harbor Perspect. Biol.* **2015**, 7, a020545.
- [8] M. Colonna, O. Butovsky, *Annu. Rev. Immunol.* **2017**, 35, 441–468.
- [9] L. Rajendran, et al., *Proc. Natl. Acad. Sci. USA* **2006**, 103, 11172–11177.
- [10] J. Skog, et al., *Nat. Cell Biol.* **2008**, 10, 1470–1476.
- [11] F. Bianco, et al., *J. Immunol.* **2005**, 174, 7268–7277.
- [12] M. Gabrielli, et al., *EMBO Rep.* **2015**, e201439668.
- [13] K. Yuyama, et al., *J. Biol. Chem.* **2014**, 289, 24488–24498.
- [14] D. Cizkova, et al., *Sci. Rep.* **2014**, 4, 7514.

- [15] H. Kettenmann, U.-K. Hanisch, M. Noda, A. Verkhratsky, *Physiol. Rev.* **2011**, *91*, 461–553.
- [16] "Isolation and Characterization of Exosomes from Cell Culture Supernatants and Biological Fluids": C. Théry, S. Amigorena, G. Raposo, A. Clayton, in *Current Protocols in Cell Biology*, Wiley, Hoboken, **2001**.
- [17] F. A. W. Coumans, et al., *Circ. Res.* **2017**, *120*, 1632–1648.
- [18] "A Protocol for Exosome Isolation and Characterization: Evaluation of Ultracentrifugation, Density-Gradient Separation, and Immunoaffinity Capture Methods": D. Greening, R. Xu, H. Ji, B. Tauro, R. Simpson, in *Proteomic Profiling* (Ed.: A. Posch), Springer, New York, **2015**, pp. 179–209.
- [19] P. Li, M. Kaslan, S. H. Lee, J. Yao, Z. Gao, *Theranostics* **2017**, *7*, 789–804.
- [20] J. Nilsson, et al., *Br. J. Cancer* **2009**, *100*, 1603–1607.
- [21] I. Helwa, et al., *PLOS ONE* **2017**, *12*, e0170628.
- [22] J. M. Street, et al., *J. Transl. Med.* **2012**, *10*, 5.
- [23] C. Théry, *F1000 Biol. Rep.* **2011**, *3*, 15.
- [24] P. K. Wallace, J. D. Tario, J. L. Fisher, S. S. Wallace, M. S. Ernstoff, K. A. Muirhead, *Cytom. Part J. Int. Soc. Anal. Cytol.* **2008**, *73*, 1019–1034.
- [25] C. A. Franzen, P. E. Simms, A. F. Van Huis, K. E. Foreman, P. C. Kuo, G. N. Gupta, *BioMed Res. Int.* **2014**, *2014*, 1–11.
- [26] V. Sokolova, et al., *Colloids Surf. B* **2011**, *87*, 146–150.
- [27] L. R. Cisneros Castillo, A.-D. Oancea, C. Stüllein, A. Régnier-Vigouroux, *Sci. Rep.* **2016**, *6*, 28375.
- [28] G. A. Calin, et al., *Proc. Natl. Acad. Sci. USA* **2008**, *105*, 5166–5171.
- [29] D. Bonci, et al., *Nat. Med.* **2008**, *14*, 1271–1277.
- [30] Q. Liu, et al., *Nucleic Acids Res.* **2008**, *36*, 5391–5404.
- [31] Y. Yang, et al., *Oncogenesis* **2017**, *6*, e351.
- [32] S. Refaie, et al., *J. Biol. Chem.* **2012**, *287*, 14703–14717.
- [33] H. Gagnon, S. Refaie, S. Gagnon, R. Desjardins, M. Salzet, R. Day, *PLoS ONE* **2013**, *8*, e61557.
- [34] M. Duhamel, et al., *Mol. Cell. Proteomics MCP* **2015**, *14*, 2857–2877.
- [35] M. Duhamel, et al., *Sci. Rep.* **2016**, *6*, 19360.
- [36] L. R. C. Castillo, A.-D. Oancea, C. Stüllein, A. Régnier-Vigouroux, *Sci. Rep.* **2016**, *6*, srep28375.

---

Manuscript received: November 3, 2017

Revised manuscript received: January 3, 2018

Accepted manuscript online: January 12, 2018

Version of record online: February 19, 2018